

## Article

# Impact of Future Development Scenario Selection on Landscape Ecological Risk in the Chengdu-Chongqing Economic Zone

Kangwen Zhu <sup>1,†</sup>, Jun He <sup>2,†</sup>, Lanxin Zhang <sup>3</sup>, Dan Song <sup>1</sup>, Longjiang Wu <sup>4</sup>, Yaqun Liu <sup>5</sup> and Sheng Zhang <sup>1,\*</sup>

<sup>1</sup> Chongqing Academy of Ecology and Environmental Sciences (Southwest Branch of Chinese Academy of Environmental Sciences), Chongqing 401147, China; zhukangwen@email.swu.edu.cn (K.Z.); sd\_sw\_edu@163.com (D.S.)

<sup>2</sup> No.107 Geological Team of the Chongqing Bureau of Geology and Mineral Exploration, Chongqing 401120, China; hj\_cqnu\_edu@163.com

<sup>3</sup> College of Earth and Environmental Sciences, Lanzhou University, Lanzhou 730000, China; zlx\_lzu\_edu@163.com

<sup>4</sup> School of Environment and Resources, Chongqing Technology and Business University, Chongqing 400060, China; wlj\_cqgsu\_edu@163.com

<sup>5</sup> Key Laboratory of Regional Sustainable Development Modeling, Institute of Geographic Sciences and Natural Resources Research, Chinese Academy of Sciences, Beijing 100101, China; liuyaqun@igsnrr.ac.cn

\* Correspondence: zs\_hky@163.com

† These authors contributed equally to this work.

**Abstract:** The management of regional eco-environmental risks is the key to promoting regional economic sustainability from the macro level, and accurate evaluation of the evolutionary trends of regional ecological risk in the future is of high importance. In order to clearly identify the possible impact of future development scenario selection for the Chengdu-Chongqing Economic Zone (C-C E Zone) on the evolution of landscape ecological risk (LER), we introduced the Patch-generating Land Use Simulation (PLUS) model to simulate land use data for the C-C E Zone from 2030 to 2050 for two scenarios: natural development (ND) and ecological protection (EP). Based on the ecological grid and landscape ecological risk index (LERI) model, the landscape ecological risk (LER) evolutionary trends seen in the C-C E Zone from 2000 to 2050 were analyzed and identified. The results showed that: (1) The PLUS model can obtain high-precision simulation results in the C-C E Zone. In the future, the currently increasing rate of land being used for construction will be reduced, the declining rates of forest and cultivated land area will also be reduced, and the amount of land being used for various purposes will remain stable going into the future. (2) This study found that the optimal size of the ecological grid in the LERI calculation of the mountainous area was 4 × 4 km. Additionally, the mean values of the LERI in 2030, 2040, and 2050 were 0.1612, 0.1628, and 0.1636 for ND and 0.1612, 0.1618, and 0.1620 for EP. (3) The hot spot analysis results showed that an area of about 49,700 km<sup>2</sup> in the C-C E Zone from 2000 to 2050 belongs to high agglomeration of LER. (4) Since 2010, the proportions of high and extremely high risk levels have continued to increase, but under the EP scenario, the high and extremely high risk levels in 2040 and 2050 decreased from 14.36% and 6.66% to 14.33% and 6.43%. Regional analysis showed that the high and extremely high risk levels in most regions increased over 2010–2050. (5) Under the ND scenario, the proportions of grids with decreased, unchanged, and increased risk levels were 15.13%, 81.48%, and 3.39% for 2000–2010 and 0.54%, 94.75%, and 4.71% for 2040–2050. These trends indicated that the proportion of grids with changed risk levels gradually decreased going into the future. This study analyzed the evolutionary trends of LER at the C-C E Zone for the ND and EP scenario. On the whole, the LER for the C-C E Zone showed an upward trend, and the EP scenario was conducive to reducing the risk. These research results can serve as a valuable data reference set for regional landscape optimization and risk prevention and control.

**Keywords:** PLUS model; scenario simulation; landscape ecological risk; ecological grid; Chengdu-Chongqing Economic Zone



**Citation:** Zhu, K.; He, J.; Zhang, L.; Song, D.; Wu, L.; Liu, Y.; Zhang, S. Impact of Future Development Scenario Selection on Landscape Ecological Risk in the Chengdu-Chongqing Economic Zone. *Land* **2022**, *11*, 964. <https://doi.org/10.3390/land11070964>

Academic Editor: Javier Martínez-López

Received: 6 June 2022

Accepted: 21 June 2022

Published: 23 June 2022

**Publisher's Note:** MDPI stays neutral with regard to jurisdictional claims in published maps and institutional affiliations.



**Copyright:** © 2022 by the authors. Licensee MDPI, Basel, Switzerland. This article is an open access article distributed under the terms and conditions of the Creative Commons Attribution (CC BY) license (<https://creativecommons.org/licenses/by/4.0/>).

## 1. Introduction

With increasing concern around ecological problems resulting from developments across the globe, there is the urgent problem of how to better implement macro-control policies to curb these issues. The management of regional eco-environmental risks is the key to promoting regional economic sustainability from the macro level. Therefore, accurate evaluation of the evolutionary trends of regional ecological risk in the future is of high importance [1]. The Chengdu-Chongqing Economic Zone (the *C-C E Zone*) is the economic core of Southwest China, playing an important role in both economic development and ecological protection [2]. On the one hand, the *C-C E Zone* provides a path for increased accessibility to inland China and improvement of the country's comprehensive strength. On the other hand, it is an important ecological barrier for the area in the upper reaches of the Yangtze River. Therefore, a method for identifying the current and future evolutionary trends for ecological risk in the large-scale range of the *C-C E Zone* is a crucial task, and one which could guide the government towards implementing ecological risk prevention and control measures and a strategy for sustainable economic development.

Generally, ecological risk assessment adopts the methods of environmental index factors, construction of evaluation index systems, and landscape ecological indices. For example, Zhang et al. analyzed the ecological risk of tetracycline antibiotics in farmland soil in Yinchuan City, China via the environmental index factor method [3]. Wee et al. studied the ecological risk of organophosphorus pesticides on the ecosystem of the Langat River using a constructed risk system [4]. Cui et al. assessed the landscape ecological risk (*LER*) in the Qinling area using a constructed landscape index [5]. In general, *LER* assessment is an effective method for risk identification, prevention, and control on a large scale while a landscape ecological risk index (*LERI*), based on ecological grid division, can reflect the *LER* status of small ecological grids [6]. The determination of the ecological grid size is a key parameter to such an assessment. An undersized grid will cut, destroy, or even change the original shape of landscape patches, but an oversized grid will lose the distribution details of landscape patches and cannot fully and truly reflect the internal *LER* situation [7]. Therefore, the determination of the ecological grid size is one of the key considerations in ecological risk assessment. In addition, research on ecological risk assessment needs to accurately predict the future *LER* of the *C-C E Zone*. Since land use change is the main basis reflecting regional landscape change, the simulation of future land use data over such a large range is another key issue. Currently, a few simulation models for land use data are widely used, including the CA Markov model [8], CLUE-S model [9], and FLUS model [10], etc. These models can obtain high simulation accuracy for small areas, but they either cannot be used or have poor results for large scales [11]. Nevertheless, we adopted the method of ecological grid division and construction of an *LERI* in this study to carry out *LER* scenario simulation and analysis in the *C-C E Zone*. In order to use this method, an accurate simulation for land use data at a large scale had to be found and the determination of the ecological grid size had to be carefully considered.

To solve the issue of accuracy in large-scale land use simulation, the Patch-generating Land Use Simulation (PLUS) model developed by the HPSCIL@CUG laboratory development team in 2020 was introduced for this study [12,13]. The typical areas were selected and the gradient division method ( $1 \times 1$  km,  $2 \times 2$  km . . . . .  $10 \times 10$  km) adopted to identify the optimal ecological grid size calculated by *LERI* in the large-scale downhill area [14,15]. Therefore, based on the land use data in 2000, 2010, and 2020, this study used the PLUS model to simulate land use data in 2030, 2040, and 2050 under natural development (*ND*) and ecological protection (*EP*) scenarios. Then, based on the identification results of the optimal size of the ecological grid, an *LERI* model, including a landscape interference index and landscape vulnerability index, was constructed to identify the *LER* evolutionary trends for the *C-C E Zone* from 2000 to 2050 to provide data in support of regional landscape optimization and ecological risk prevention and control.

## 2. Materials and Methods

### 2.1. Study Area

The C-C E Zone is located in the southwest of China, and it includes Chengdu, Deyang, Mianyang, Meishan, Ziyang, Suining, Leshan, Ya'an, Zigong, Luzhou, Neijiang, Nanchong, Yibin, Dazhou, and Guang'an in Sichuan Province and Wanzhou, Fuling, the main urban areas of Chongqing (Yuzhong, Dadukou, Jiangbei, Shapingba, Jiulongpo, Nan'an, Beibei, Yubei, Banan), Changshou, Jiangjin, Hechuan, Yongchuan, Nanchuan, Qijiang (including Wansheng), Tongnan, Tongliang, Dazu (including Shuangqiao), Rongchang, Bishan, Liangping, Fengdu, Dianjiang, Zhongxian, Kaizhou, Yunyang, and Shizhu in Chongqing, with an area of about  $20.6 \times 10^4 \text{ km}^2$  [2]. The C-C E Zone is an agglomeration of important areas for the population, towns, and industry in western China. With rapid economic development has come urban expansion in the region, which has put pressure on ecological spaces. It is crucial to accurately and effectively lay out production, living, and ecological spaces, and this can be assisted through projection of the evolutionary trends of *LER* in the region. Therefore, *LER* analysis and the simulation of long-term series in this region is of great importance as it can promote regional ecological risk prevention and control and sustainable economic development.

### 2.2. Data Sources

The data used in the study included: the land use data regarding the C-C E Zone in 2000, 2010, and 2020 from the Resource and Environmental Science Data Center of Chinese Academy of Sciences (<https://www.resdc.cn/Default.aspx> (accessed on 1 December 2021)) [16] and globeland30 (<http://www.globallandcover.com> (accessed on 15 December 2021)); NDVI data and soil type data from the Resource and Environmental Science Data Center of Chinese Academy of Sciences (<https://www.resdc.cn/Default.aspx> (accessed on 1 December 2021)); terrain data from geospatial data cloud website (<http://www.gscloud.cn/> (accessed on 10 December 2021)); and road data from OpenStreetMap. The resolution of the above data was resampled to 30 m.

### 2.3. Methods

Based on the land use data for the C-C E Zone in 2000, 2010, and 2020, we used the PLUS model to simulate land use data from 2030 to 2050 under different scenarios (i.e., *ND* and *EP*). The evolutionary trends and characteristics of *LER* from 2000 to 2050 were evaluated using ecological grids and the *LERI* model, and then further analyzed using ArcGIS software. These results could provide support for regional landscape optimization and risk prevention and control in the future (Figure 1).

Land use data from the C-C E Zone were collected from 2000 to 2020, including DEM, slope, NDVI, soil type, distance from water area, distance from a primary road, distance from a secondary road, distance from a main road, distance from an expressway, distance from other roads, and distance from a railway line as the driving factors of land use change, and water area as a limiting factor of land use change. Firstly, the feasibility and accuracy of the PLUS model were verified for a 30 m resolution land use data simulation within the C-C E Zone. Land use data for the C-C E Zone were then simulated for 2030, 2040, and 2050 for both the *ND* and *EP* scenarios. Finally, the *LERI* model was used to analyze the *LER* temporal and spatial evolution for the C-C E Zone from 2000 to 2050 under the two scenarios to provide data support for regional urban development and land layout and ecological risk prevention and control in the future.

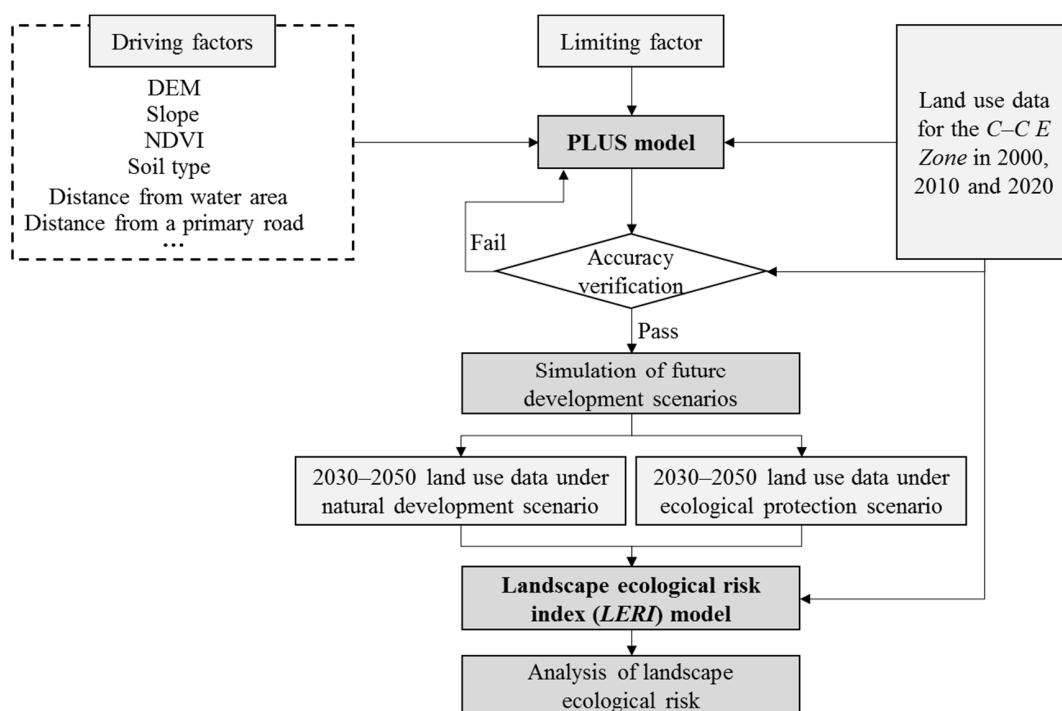


**Figure 1.** Research framework map.

### 2.3.1. PLUS Model

The PLUS model is a patch-generated land use change simulation model developed by the HPSCIL@CUG laboratory development team. Compared with other commonly used models (i.e., the CLUE-S and CA-Markov models), PLUS has the following advantages: (1) The land expansion analysis strategy applied by the model can better demonstrate the incentives behind various land use changes. As an example, the random forest algorithm is used to mine the factors of various land use expansion and driving forces one by one to obtain the development probability of various land uses and the contribution of driving factors to various land use expansion. This strategy combines the advantages of the existing transformation analysis strategy and pattern analysis strategy, retains the ability of the model to analyze the mechanism of land use change in a certain period of time, and has better interpretability. (2) It contains a new multi-class seed growth mechanism, which can better simulate the patch-level change in multi-class land use. Combined with random seed generation and a threshold decreasing mechanism, the model can dynamically simulate the automatic generation of patches under the constraint of development probability [12,13].

The simulation of the *C-C E Zone* is divided into two steps: (1) Based on the land use data from 2000 to 2010, the data for 2010 and 2020, respectively, were simulated, and then the real data of 2010 and 2020 were used for accuracy analysis. A kappa coefficient is usually used as the basis for accuracy analysis. If the kappa coefficient is higher than 0.75, it means that the model achieves a highly consistent level [11]. (2). On the premise that the simulation accuracy met the requirements, the land use data for 2030, 2040, and 2050 were simulated for the *ND* and *EP* scenarios. The future demand for each land use type (i.e., the area of each land use type) under the *ND* scenario was predicted by a Markov chain module integrated with the PLUS model. The demand under the *EP* scenario was calculated by reducing the area increase or decrease in various land use types by 20% under the *ND* scenario.

### 2.3.2. Determination of the Optimal Size of the Ecological Grid

The ecological grid will split the original natural ecosystem of the region and have a certain impact on the evaluation and analysis of local *LER*. Different sizes of the ecological

grid will produce different results of *LER*; when a too large or too small ecological grid is used, it will be difficult to reflect the real situation of *LER*.

Based on the ecological grid size delimitation results of existing scholars (Table 1), this study was based on ArcGIS software and the gradient division method ( $1 \times 1$  km,  $2 \times 2$  km,  $3 \times 3$  km,  $4 \times 4$  km,  $5 \times 5$  km,  $6 \times 6$  km,  $7 \times 7$  km,  $8 \times 8$  km,  $9 \times 9$  km,  $10 \times 10$  km) to divide the area into several ecological grids and code each ecological grid. The *LERI* of each grid was calculated one by one, then the Kriging method was used for interpolation, and the interpolation results were graded to obtain the spatial classification map of *LER*. The *LERI* of each grid was calculated using ArcGIS modeling and the FRAGSTATS batch processing method, and the change in the value range of *LERI* under each ecological grid size scenario was analyzed to determine the optimal size of the regional ecological grid [14,15].

**Table 1.** The size of ecological grid used in previous studies.

Research's Regional	Area of Research's Regional (Unit: km <sup>2</sup> )	Resolution of Land Use Data (Unit: m)	Size of Ecological Grid (Unit: km)
Nanchang, China [17]	7402.36	30	$3 \times 3$
Western of Jilin, China [18]	$4.69 \times 10^4$	30	$3 \times 3$
Western of Henan, China [19]	$2.71 \times 10^4$	30	$5 \times 5$
District of Xiajiang, Wuhan, China [20]	2018	30	$2 \times 2$
Lower reaches of Tarim River [21]	$1.28 \times 10^4$	30	$3 \times 3$
District of Wanzhou, Chongqing, China [22]	3456.55	50	$2 \times 2$
District of Jiangjin, Chongqing, China [23]	3217.77	30	$3 \times 3$
Three Gorges Reservoir area [14]	$5.85 \times 10^4$	30	$4 \times 4$

### 2.3.3. Building the Landscape Ecological Risk Index (*LERI*) Model

Landscape ecological risk (*LER*) refers to the possible adverse consequences from the interaction between landscape patterns and ecological processes under the influence of natural or human factors, which can be defined as the combination of risk probability and the degree of landscape lost [24]. Based on existing research results and the factors from the area being studied, the *LERI* calculation model was constructed. The calculation formulas are as follows:

$$LERI_k = \sum_{i=1}^n \frac{A_{ki}}{A_k} \sqrt{U_i \times F_i} \quad (1)$$

$$U_i = aC_i \times bS_i \times cD_{oi} \quad (2)$$

$$C_i = \frac{n_i}{A_i}, S_i = \frac{A}{2A_i} \sqrt{\frac{n_i}{A}}, D_{oi} = \frac{2 \ln \frac{P_i}{4}}{\ln A_i} \quad (3)$$

In these formulas,  $n$  is the number of landscape types,  $A$  is the total area,  $A_{ki}$  is the area of landscape type  $i$  in the  $k$ -th sample area,  $A_i$  is the area of landscape type  $i$ ,  $A_k$  is the total area of the  $k$ -th sample area,  $n_i$  is the number of patches of landscape type  $i$ , and  $p_i$  is the perimeter of the landscape type  $i$ .  $U_i$  is the landscape interference index, which reflects the degree to which landscape is lost in a certain area after external interference.  $C_i$ ,  $S_i$ , and  $D_{oi}$  are the landscape fragmentation index (indicating the degree of spatial division of the landscape type in a certain time), the landscape separation index (indicating the degree of separation of different patches in the landscape type), and the landscape sub dimension index (indicating the complexity of the shape of the landscape patch). The value range is 1–2, with larger values indicating greater complexity in the shape of the landscape patch.  $a$ ,  $b$ , and  $c$  represent the weight of each index, and the values are 0.5, 0.3, and 0.2, respectively [25].  $F_i$  is the landscape vulnerability index, which reflects the ability

of a landscape type to resist external interference and its sensitivity to external changes. Referring to relevant studies [26], the six landscape types of construction land, forest land, grassland, cultivated land, water, and other land are assigned as 1–6, respectively. Normalized to  $F_i$ , the greater the value, the weaker the ability to cope with interference.

#### 2.3.4. Calculation and Classification of Landscape Ecological Risk

Using ArcGIS software and the Model Builder tool, this study calculated the *LERI* of 12,834 ecological grids in the *C-C E Zone* from 2000 to 2050 one by one and obtained the long-term series *LERI* distribution data. In order to ensure the spatial continuity of the data, the Kriging tool in ArcGIS software was used to spatially interpolate the *LERI* value for each ecological grid [15]. At the same time, in order to ensure comparability between multi-period data, based on the interpolation results of the *LERI* value in 2020, *LER* in 2020 was divided into five levels: no risk, low risk, medium risk, high risk, and extremely high risk, using the natural breakpoint method. The value range of each grade was determined according to this standard, as was the *LERI* value in other periods.

#### 2.3.5. Getis-Ord $G_i^*$ Analysis

The Getis-Ord  $G_i^*$  analysis is widely used in crime analysis, epidemiology, and economic geography to identify spatial gathering of high values (hot spots) and low values (cold spots) with statistical significance [27]. In a Getis-Ord  $G_i^*$  analysis, the  $z$  score,  $p$  values, and confidence intervals ( $G_i$ \_Bin) are employed to create a new output class for each element in the input element class. Here, the  $z$  score and  $p$  values can help to judge whether the null hypothesis can be rejected while the  $G_i$ \_Bin field is used to identify statistically significant hot and cold spots. The elements in the confidence interval of [+3, −3] have a statistical significance with a confidence level of 99% while those in the confidence interval of [+2, −2] have a statistical significance with a confidence level of 95%, and those in the confidence interval of [+1, −1] have a statistical significance with a confidence level of 90%. When the element gathering of the  $G_i$ \_Bin field is 0, there is no statistical significance.

### 3. Results

#### 3.1. Simulation Accuracy Analysis of Land Use Data

The PLUS model was used to simulate the land use data. The accuracy analysis results showed that the kappa coefficient of the simulated 2010 data based on the 2000 data was 0.81, and the kappa coefficient of the simulated 2020 data based on the 2010 data was 0.82. The kappa coefficients were higher than 0.75, indicating that the PLUS model had good simulation effects for the *C-C E Zone*, and the simulation accuracy had a high level of consistency. This meant that the model could be used to simulate future land use data for the *C-C E Zone*.

#### 3.2. Trend Analysis of Land Use Evolution from 2000 to 2050

The evolution of land use in the *C-C E Zone* from 2000 to 2050 indicated obvious trends in the region, as shown in Figure 2. The overall growth rate of construction land decreased slowly, showing a multipolar and multipoint growth trend. From 2000 to 2010 and from 2010 to 2020, the area increased by 496.96 and 4427.55 km<sup>2</sup>, respectively. Under the *ND* scenario, it was projected to increase by 1990.66, 3782.9, and 1172.54 km<sup>2</sup> in 2020–2030, 2030–2040, and 2040–2050, respectively. Under the *EP* scenario, the increases would be 1592.53, 1433.79, and 1292.44 km<sup>2</sup> in 2020–2030, 2030–2040, and 2040–2050, respectively. In general, the increase in construction land under the *EP* scenario was reduced compared to the *ND* scenario by 4.39%, 21.38%, and 18.74% in 2030, 2040, and 2050, respectively. In terms of spatial characteristics, the main urban areas of Chongqing and Chengdu were the main growth poles, and Mianyang, Deyang, Suining, Wanzhou, Nanchong, Luzhou, Yongchuan, Changshou, and Fuling were the secondary growth poles. In addition, forest land showed an increasing trend in the beginning and then decreased. The forest land area increased by 3.19% from 2000 to 2010 and decreased by 2.11% from 2010 to 2020. After that, the

forest land area showed a slow downward trend, but the area increased from 2040 to 2050 under the *EP* scenario. Compared with the *EP* scenario in 2030, 2040, and 2050, the total area of forest land in the *ND* scenario increased by 0.04%, 0.28%, and 1.48%, respectively. The cultivated land showed a slightly increasing trend (0.26%) during 2000–2010 and then gradually decreased by 4.11% from 2010 to 2020. Under the *ND* scenario, cultivated land decreased by 1.86%, 3.18%, and 1.01%, respectively, during 2020–2030, 2030–2040, and 2040–2050. The decreases in the cultivated land area under the *EP* scenario saw this land type reduced to 429.84, 2567.43, and 2333.3 km<sup>2</sup> in 2030, 2040, and 2050, respectively, but these values were still higher than those under the *ND* scenario. The water area showed a trend of “decrease-increase-stability”, with a decrease of 4.96% during 2000–2010 followed by an increase of 30.13% during 2010–2020. During 2020–2030, the water area under the *ND* and *EP* scenarios increased by 3.92% and 3.32%, respectively, while the change between 2030–2040 and 2040–2050 was limited. Grassland and other land types were randomly distributed in mountainous areas, and the changes in the total area were relatively stable. Therefore, the growth rate of construction land will be reduced, the decline in forest land and cultivated land area will be reduced, and all types of land areas will gradually stabilize in the future. Meanwhile, the ecological land area under the *EP* scenario was significantly higher than that under the *ND* scenario.

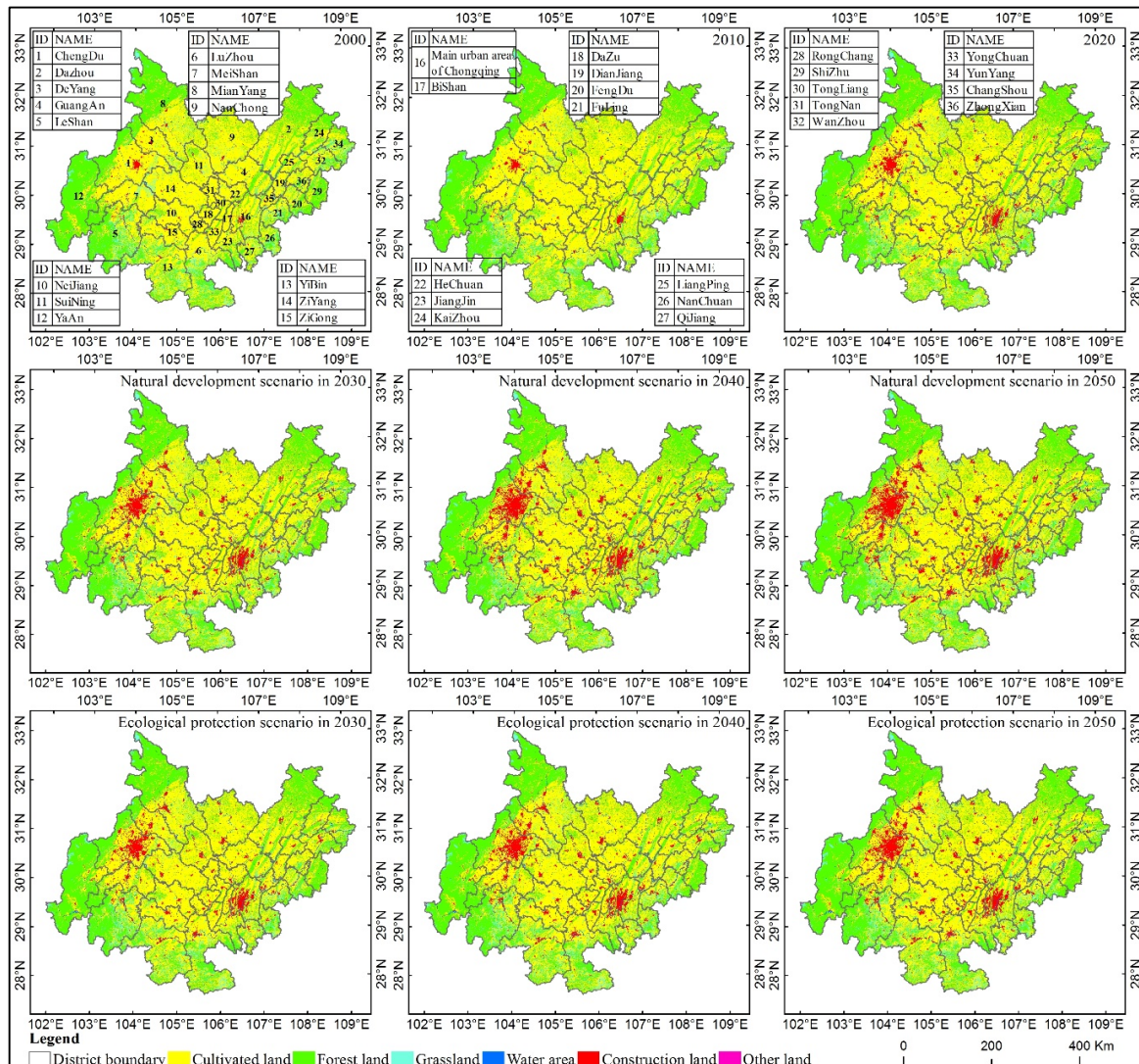


Figure 2. Distribution of the simulation results of land use data in the C-C E Zone from 2030 to 2050.

### 3.3. Analysis of the Optimal Size of the Ecological Grid

We selected the Three Gorges Reservoir area in C-C E Zone as a typical area to determine the optimal scale of the ecological grid, and the total area, topography, and land use types of this area were representative. We divided the study area into 60,216, 15,459, 7031, 4049, 2638, 1869, 1405, 1091, 886, and 719 ecological grids according to the grid size of  $1 \times 1$ ,  $2 \times 2$ ,  $3 \times 3$ ,  $4 \times 4$ ,  $5 \times 5$ ,  $6 \times 6$ ,  $7 \times 7$ ,  $8 \times 8$ ,  $9 \times 9$ , and  $10 \times 10$  km. We calculated the *LERI* under different sizes of the ecological grid in 2020, and obtained the curve of *LERI* under each ecological grid (Figure 3). The results show that the average value of *LERI* was between 0.1649 and 0.1688, and the change in the ecological grid size had little impact on the average value, indicating that the size of the ecological grid has little impact on the *LER* of the whole region. We extracted the maximum and minimum values of *LERI*, and found that the maximum and minimum values of *LERI* began to stabilize at  $4 \times 4$  km. When the ecological grid was less than  $4 \times 4$  km, the difference between them showed an obvious decreasing trend, and when the ecological grid was greater than  $4 \times 4$  km, the difference between them tended to stabilize. In regional *LERI* research, the size of the ecological grid will have a great impact on the results. Too small an ecological grid will make the spatial expression too delicate, thus covering up the overall spatial law and causing a lot of redundant computing work, and too large an ecological grid will lead to the loss and misjudgment of the spatial law. Therefore, in order to truly reflect the temporal and spatial differentiation characteristics of regional *LERI*, and comprehensively consider the variation law of the *LERI* value with the size of the ecological grid, it was determined that based on the resolution of 30 m land use data in the C-C E Zone, the optimal scale of the ecological grid in the *LERI* calculation was  $4 \times 4$  km.

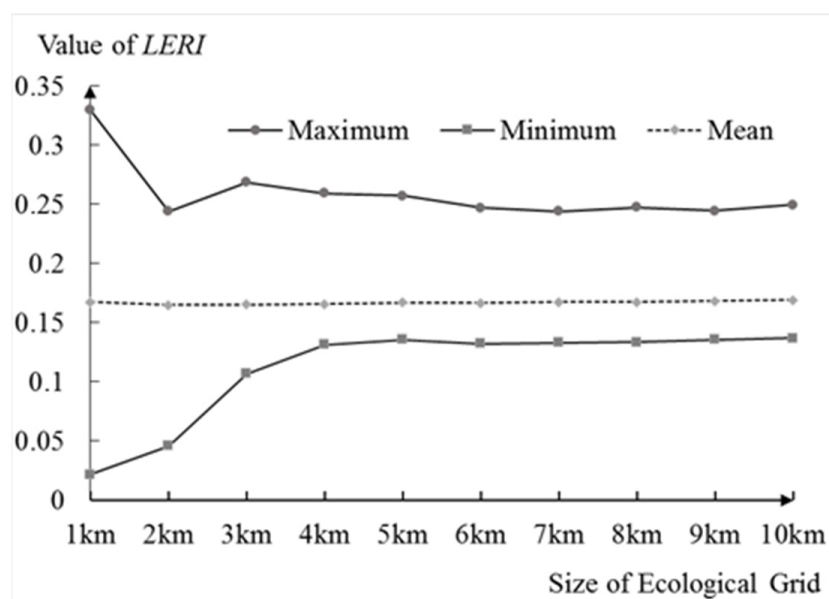


Figure 3. *LERI*'s value under different sizes of the ecological grid in 2020.

### 3.4. Analysis of the Calculation Results of LERI

The average values of the *LERI* in 2000, 2010, and 2020 were 0.1617, 0.1588, and 0.1592, respectively. The average values of the *LERI* under the *ND* scenario were 0.1612, 0.1628, and 0.1636, respectively, while under the *EP* scenario, the average values were 0.1612, 0.1618, and 0.1620, respectively, in 2030, 2040, and 2050. The mean value of the *LERI* in the *EP* scenario was significantly lower than that in the *ND* scenario, indicating that the *EP* development scenario was valuable for reducing regional *LER*.

In terms of the *LERI* changes in each period, the number of ecological grids with increased, unchanged, and decreased *LER* was 5058, 272, and 7504, respectively, during 2000–2020. The sum of the *LERI* for increased and decreased ecological grids was 20.7360 and

53.0439, respectively, while the average of the *LERI* increased and decreased ecological grids was 0.0410 and 0.0071, respectively. Generally, *LER* is decreasing in the studied area overall, but increases were observed in some ecological grids. During 2020–2050, under both the *ND* and *EP* scenarios, the number of ecological grids with increased, unchanged, and decreased *LER* was 9046, 622, and 3166 for the former and 7403, 595, and 4836 for the latter. The sum of the *LERI* of increased and decreased ecological grids was 59.5840 and 3.1447 for the former and 40.8484 and 4.3616 for the latter. The results showed that *LER* for 2020–2050 showed an increasing trend as a whole, and the *EP* scenario could significantly reduce the regional *LER*.

### 3.5. Hot Spot Analysis of *LER*

The hot spot analysis results of *LER* in the *C-C E Zone* from 2000 to 2050 suggested no significant change in the space of high-risk and low-risk agglomeration areas for each period, indicating that the overall layout of various land uses was relatively stable (Figure 4). From 2000 to 2050, the area with the highest concentration of *LER* accounted for 21.13–22.06%, indicating that the area with the highest concentration of *LER* was about 49,700 km<sup>2</sup>. Using 2020 as an example, the high-value agglomeration areas of *LER* were mainly distributed in the southeast of Mianyang, the southeast of Deyang, the east of Leshan, the junction of Neijiang-Zigong, Yibin, Luzhou, the south of Jiangjin, Qijiang, the south of Banan, the south of Fuling, Fengdu, the north of Shizhu, the north of Zhongxian, the south of Wanzhou, the south of Yunyang, etc. The low-value agglomeration areas of *LER* were mainly distributed in the west and middle of the *C-C E Zone*, including the northwest of Mianyang, the northwest of Deyang, Chengdu, Meishan, Ya'an, Ziyang, Suining, the south of Guang'an, the east of Neijiang, the northeast of Dazhou, Rongchang, Dazu, Tongnan, the north of Zigong, Hechuan, Bishan, etc. From the degree of change in agglomeration, there was an upward trend in the degrees of agglomeration for high-value areas of *LER* in the north and southeast of Chengdu, the west and southeast of Nanchong, etc. In contrast, there was a downward trend in the degree of agglomeration for high-value areas of *LER* in Yunyang, Wanzhou, Shizhu, Liangping, Zhongxian, etc. In addition, downward trends in the degrees of agglomeration for low-value areas of *LER* were observed in the Mianyang, Deyang, Chengdu, Meishan, etc., while upward trends in the degrees of agglomeration for low-value areas of *LER* were observed in the southeast of Nanchong and west of Dazhou, etc.

### 3.6. Analysis of the Grade Evolutionary Trends for *LER* from 2000 to 2050

#### 3.6.1. Overall Analysis of the Grade Evolutionary Trends for *LER* in the *C-C E Zone*

In order to enhance the comparability between multi-period data, the natural break-point method was used to grade *LER* in 2020 in ArcGIS, and the interpolation results of the *LERI* were divided into five levels: no risk (*LERI* value, 0–0.1456), low risk (0.1456–0.1631), medium risk (0.1631–0.1824), high risk (0.1824–0.2034), and extremely high risk (0.2034–1).

The proportions of high and extremely high risk levels for the *C-C E Zone* in 2000, 2010, and 2020 were 14.21%, 13.47%, and 13.75% for the former and 8.14%, 5.63%, and 5.89% for the latter, indicating that the *LER* level decreased from 2000 to 2010, and then increased from 2010 to 2020 (Table 2). Under the *ND* scenario, the high and extremely high risk levels for the *C-C E Zone* have continued to increase since 2010. Under the *EP* scenario, the high and extremely high risk levels for the *C-C E Zone* have continued to increase during 2010–2040, but there was a downward trend during 2040–2050. The high and extremely high risks decreased from 14.36% to 14.33% in 2040, and from 6.66% to 6.43% in 2050. Therefore, the results suggested that the *EP* scenario was beneficial for environmental protection in the long term and could reduce the proportion of high and extremely high risk levels of *LER* in the region.

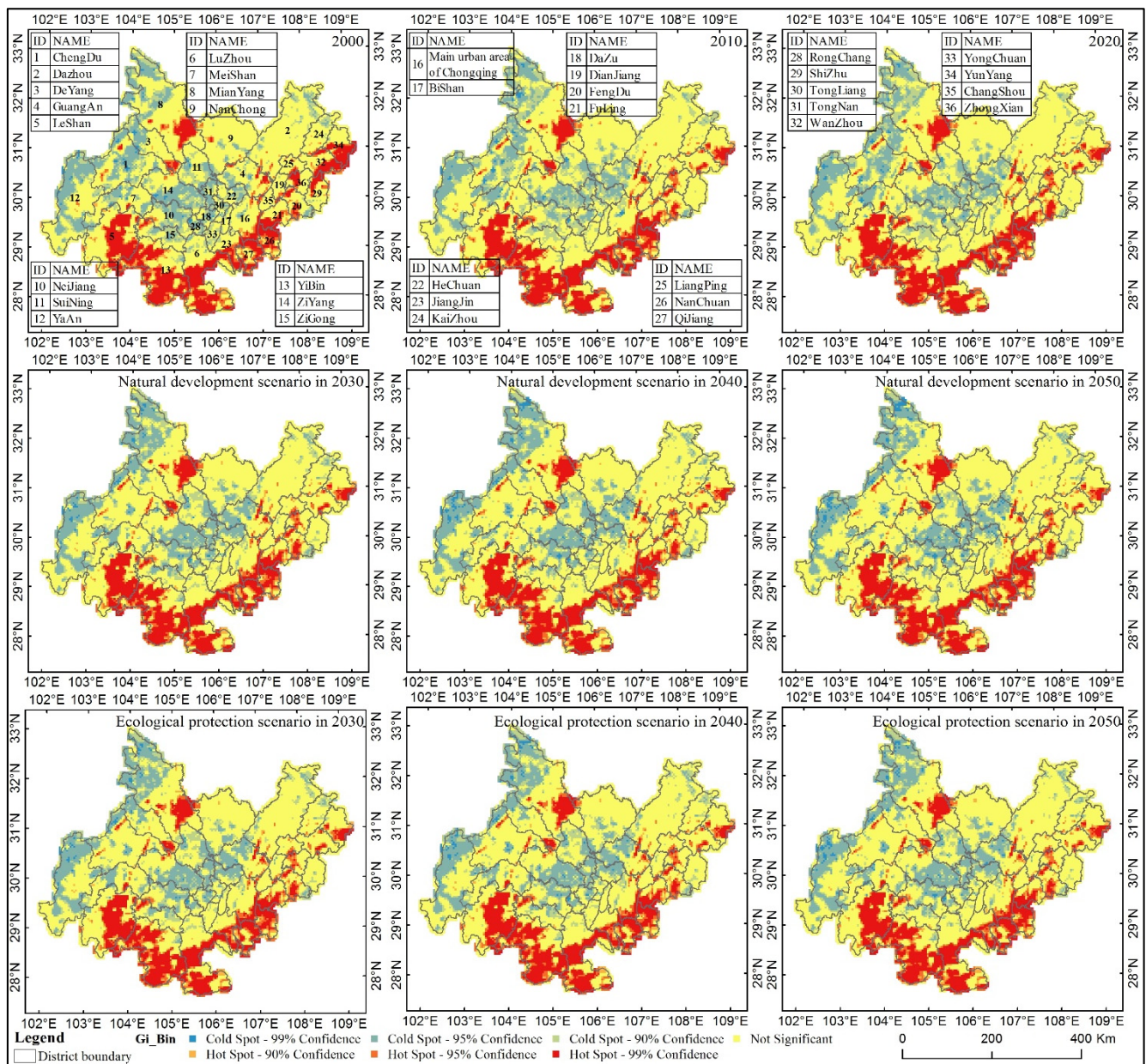


Figure 4. Distribution of hot spots of LERI from 2000 to 2050.

Table 2. Statistical table of LER's proportion of each grade from 2000 to 2050.

Level\Period	2000	2010	2020	ND Scenario			EP Scenario		
				2030	2040	2050	2030	2040	2050
No risk	36.18	40.97	40.33	33.57	29.31	27.47	33.68	31.71	30.37
Low risk	24.13	22.67	23.16	27.6	29.12	30.06	27.34	28.59	29.43
Medium risk	17.34	17.26	16.87	18.12	20.02	20.13	18.36	18.68	19.44
High risk	14.21	13.47	13.75	14.26	14.52	14.67	14.26	14.36	14.33
Extremely high risk	8.14	5.63	5.89	6.45	7.03	7.67	6.36	6.66	6.43

### 3.6.2. Evolutionary Trend Analysis of the LER Levels in Various Regions

For LER, we usually focus on high- and extremely-high-risk areas (Table 3). The statistical analysis shows that the proportions of high and extremely high risk in most areas decreased from 2000 to 2010, except in Chengdu, Deyang, Meishan, Neijiang, and

Fuling. During 2010–2050, most regions under the *ND* scenario showed a trend of increasing proportions of high and extremely high risk, among which Fengdu, Fuling, Changshou, and Nanchuan had the greatest increases, by 17.76%, 15.35%, 11.76%, and 10.09%, respectively. During the period of 2010–2050, although the overall high and extremely high levels of risk in the *EP* scenario showed an increasing trend, these levels decreased in 22 regions during the period of 2040–2050, including in Dazhou, Deyang, Guang’an, Lashan, Luzhou, etc. In addition, there was no high- or extremely-high-level risk distribution throughout Ya’an, Bishan, Dazu, Hechuan, Rongchang, Tongliang, Tongnan, and Yongchuan, indicating that *LER* in these regions is generally low. Except for the fact that Ya’an is located in the west of the *C-C E Zone*, the other regions are located in the Chengdu-Chongqing transition zone. Furthermore, these regions are the main contributors to low *LER* due to having a medium level of economic development and flat terrain and a dense proportion of agriculture. In general, the proportion of high and extremely high risk in each region is significantly lower in the *EP* scenario than the *ND* scenario.

**Table 3.** Statistical table of high and extremely high risk proportions of *LER* in each region.

Region\Period	2000	2010	2020	<i>ND</i> Scenario			<i>EP</i> Scenario		
				2030	2040	2050	2030	2040	2050
Chengdu	1.93	1.93	2.02	2.89	4.34	5	2.76	3.37	3.53
Dazhou	1.77	1.32	1.55	1.75	2.15	2.52	1.74	1.86	1.81
Deyang	11.26	11.65	11.46	12	12.45	12.98	11.89	12.19	12.01
Guangan	7.12	5.23	4.63	5.42	5.92	6.39	5.33	5.61	5.25
Leshan	47.4	47.09	47.1	48.31	49.68	52.64	48.17	49.01	47.96
Luzhou	62.4	52.33	55.32	56.65	57.64	59.32	56.37	56.98	56.5
Meishan	3.51	4.12	4.09	4.32	5.09	5.51	4.29	4.5	4.8
Mianyang	12.57	10.92	11.2	12.59	13.45	13.95	12.8	12.89	12.59
Nanchong	4.71	2.45	2.49	2.77	2.84	2.98	2.72	2.81	2.62
Neijiang	5.84	6.1	6.11	6.33	6.84	7.22	6.31	6.49	6.39
Suining	0.88	0.69	0.8	0.79	0.81	0.9	0.78	0.8	0.81
Yaan	0.36	0	0	0	0	0	0	0	0
Yibin	79.16	77.68	78.4	80.74	82.41	83.37	80.64	81.41	81.25
Ziyang	0.56	0.53	0.58	1.11	1.44	1.88	1	1.13	1.18
Zigong	10.65	10.83	11.04	11.51	11.81	12.37	11.42	11.59	11.52
Main urban area of Chongqing	21.7	18.83	19.99	22.97	23.69	24.43	22.91	23.12	23.1
Bishan	0	0	0	0	0	0	0	0	0
Dazu	0	0	0	0	0	0	0	0	0
Dianjiang	9.57	3.72	3.39	6.75	7.87	9.16	6.1	7.15	5.66
Fengdu	42.81	35.02	43.38	46.72	49.48	52.78	46.04	47.83	46.37
Fuling	58.68	59.31	61.65	68.1	72.11	74.66	67.74	69.3	68.15
Hechuan	0	0	0	0	0	0	0	0	0
Jiangjin	46.82	41.83	42.5	43.26	44.72	45.53	43.33	43.87	43.91
Kaizhou	3.87	0.03	0.06	0.1	0.13	0.2	0.09	0.11	0.1
Liangping	19.54	10.93	12.23	13.84	12.83	13.24	13.46	14.21	12.3
Nanchuan	91.18	81.23	85.23	87.82	89.49	91.32	87.21	88.61	88.44
Qijiang	80.32	77.21	78.66	82.97	84.77	86.92	82.63	83.89	82.7
Rongchang	0	0	0	0	0	0	0	0	0
Shizhu	23.11	0.26	0.19	0.22	0.35	0.63	0.22	0.29	0.32
Tongliang	0	0	0	0	0	0	0	0	0
Tongnan	0	0	0	0	0	0	0	0	0
Wanzhou	50.64	12.91	14.48	15.64	17.07	18.23	15.5	16.17	15.54
Yongchuan	0	0	0	0	0	0	0	0	0
Yunyang	59.84	33.21	31.91	33.07	35.82	36.39	32.71	33.91	33.5
Changshou	14.14	12.3	9.32	17.46	21.65	24.06	16.41	19.03	17.65
Zhongxian	33.98	22.68	25.46	26.7	28.51	30.1	26.26	27.06	26.75
<i>C-C E Zone</i>	22.35	19.1	19.65	20.71	21.55	22.34	20.62	21.02	20.76

### 3.6.3. Analysis of the *LER* Rates of Change in Various Regions

To evaluate the level of change in *LER* for the *C-C E Zone*, the rate of change was examined in relation to the change in high and extremely high risk levels (Table 4). During 2000–2010, the proportions of high and extremely high risk decreased in 24 regions while the proportions were stable in 8 regions, and increased in 4 regions. Wanzhou, Yunyang, and Shizhu had the greatest rate of decline, reaching  $-3.773$ ,  $-2.663$ , and  $-2.285$  per year, respectively. During 2010–2020, the proportions of high and extremely high risk decreased in 7 regions but were stable and increased in 8 and 21 regions, respectively. Fengdu, Nanchuan, and Luzhou had the highest rates of increase, reaching 0.836, 0.4, and 0.299 per year, respectively. Under the *ND* scenario, Suining was the only region that showed a decrease in the high and extremely high risk proportions during 2020–2030. These proportions were stable across eight regions, with the top increases observed in Changshou (0.814 per year), Fuling (0.645 per year), and Qijiang (0.431 per year). There were increasing trends in 27 regions for the proportions of both high and extremely high risk levels. Similarly, the majority of the regions (27 out of 36) showed a decreasing proportion of high and extremely high risk during 2030–2040 while Liangping was the only region with a decreasing trend ( $-0.101$  per year), and another eight regions, including Changshou (0.419 per year), Fuling (0.401 per year), Fengdu (0.276 per year), etc., showed increasing trends in the proportion of high and extremely high risk. During 2040–2050, these proportions were stable in 8 regions while they increased in another 28 regions, with the highest increases found in Fengdu (0.330 per year), Leshan (0.296 per year), and Fuling (0.255 per year). In conclusion, the risk levels in Fuling, Fengdu, and Changshou continued to increase from 2000 to 2050, with risk increase rates of 0.3196, 0.1994, and 0.1984 per year, respectively. Fuling is one of the strongest economies in Chongqing, with its GDP being among the top five in the area. Fuling has a complex terrain, developed agriculture, and frequent interference due to human activities, which is the main reason for its high *LER*. Fengdu is a typical area of this region composed of parallel folded mountains. The mountains and hills in Fengdu are widely distributed, and narrow flat dams exist only in valleys, which is the main reason for its high *LER*. As a national economic and technological development zone, Changshou has seen rapid economic development and is close to the main city of Chongqing. Changshou's economic development and intense human interference have remained at a high level for a long time, which is the main reason for its high *LER*.

### 3.6.4. Analysis of the Evolutionary Trends for *LER* Levels at the Grid Scale

The risk-level changes in each grid for different periods were analyzed by a transfer matrix method. Based on the changes in risk level, the grids were divided into several groups: severe decline ( $-3$ ), moderate decline ( $-2$ ), slight decline ( $-1$ ), no change (0), slight rise (1), moderate rise (2), and severe rise (3) (Figure 5). From 2000 to 2010, the number of grids with decreased, unchanged, and increased risk levels accounted for 15.13%, 81.48%, and 3.39% of the area, among which the grids with increased risk levels were mainly located at the junction of Fengdu-Shizhu, the southeast of Shizhu, the east of Changshou, the east of Mianyang, the junction of Chengdu-Ya'an, the middle of Meishan, the east of Chengdu, Deyang, Dazhou, Luzhou, the main urban area of Chongqing, etc. The grids with reduced risk levels were mainly located in the area of Shizhu-Wanzhou-Yunyang-Kaizhou, the area of Guang'an-Nanchong-Suining-Mianyang-Deyang, Chengdu, Ya'an, Meishan, Ziyang, Yibin, Luzhou, Jiangjin, Bishan, the main urban area of Chongqing, Nanchuan, etc. From 2010 to 2020, the number of grids with decreased, unchanged, and increased risk levels accounted for 1.74%, 94.95%, and 3.31%, among which the grids with increased risk levels were mainly located at the junction of Fengdu-Shizhu, southwest of Nanchong, west of Ziyang, south of Luzhou, etc. The grids with reduced risk levels were mainly located at the junction of Leshan-Meishan, etc. Under the *ND* scenario, during 2020–2030, the number of grids with decreased, unchanged, and increased risk levels accounted for 1.74%, 94.95%, and 3.31% of the area, among which the grids with increased risk levels were

mainly located in Meishan, Chengdu, Deyang, Suining, the main urban area of Chongqing, Yongchuan, etc. During 2030–2040, the proportion of grids with changes in the risk level decreased. The number of grids with decreased, unchanged, and increased of risk levels accounted for 0.30%, 91.00%, and 8.70% of the area, and small rises in the degrees were only concentrated in Deyang, Chengdu, Mianyang, the area of Tongliang-Hechuan-Bishan-Dazu-Yongchuan, etc. During 2040–2050, the proportion of grids with risk-level changes continued to decrease. The number of grids with decreased, unchanged, and increased risk levels accounted for 0.54%, 94.75%, and 4.71% of the area, and small rises in the degrees were only concentrated in Dazhou, Nanchong, Ziyang, Mianyang, etc. The evolutionary trends for the risk levels in each period under the *EP* scenario were consistent with those in the *ND* scenario, but the decline in the proportions of risk levels is higher than those in the *ND* scenario.

**Table 4.** Rate of change in the high and extremely high risks of *LER* in each region.

Region\Period	2000–2010	2010–2020	<i>ND</i> Scenario			<i>EP</i> Scenario		
			2020–2030	2030–2040	2040–2050	2020–2030	2030–2040	2040–2050
Chengdu	0	0.009	0.087	0.145	0.066	0.074	0.061	0.016
Dazhou	−0.045	0.023	0.02	0.04	0.037	0.019	0.012	−0.005
Deyang	0.039	−0.019	0.054	0.045	0.053	0.043	0.03	−0.018
Guangan	−0.189	−0.06	0.079	0.05	0.047	0.07	0.028	−0.036
Leshan	−0.031	0.001	0.121	0.137	0.296	0.107	0.084	−0.105
Luzhou	−1.007	0.299	0.133	0.099	0.168	0.105	0.061	−0.048
Meishan	0.061	−0.003	0.023	0.077	0.042	0.02	0.021	0.03
Mianyang	−0.165	0.028	0.139	0.086	0.05	0.16	0.009	−0.03
Nanchong	−0.226	0.004	0.028	0.007	0.014	0.023	0.009	−0.019
Neijiang	0.026	0.001	0.022	0.051	0.038	0.02	0.018	−0.01
Suining	−0.019	0.011	−0.001	0.002	0.009	−0.002	0.002	0.001
Yaan	−0.036	0	0	0	0	0	0	0
Yibin	−0.148	0.072	0.234	0.167	0.096	0.224	0.077	−0.016
Ziyang	−0.003	0.005	0.053	0.033	0.044	0.042	0.013	0.005
Zigong	0.018	0.021	0.047	0.03	0.056	0.038	0.017	−0.007
Main urban area of Chongqing	−0.287	0.116	0.298	0.072	0.074	0.292	0.021	−0.002
Bishan	0	0	0	0	0	0	0	0
Dazu	0	0	0	0	0	0	0	0
Dianjiang	−0.585	−0.033	0.336	0.112	0.129	0.271	0.105	−0.149
Fengdu	−0.779	0.836	0.334	0.276	0.33	0.266	0.179	−0.146
Fuling	0.063	0.234	0.645	0.401	0.255	0.609	0.156	−0.115
Hechuan	0	0	0	0	0	0	0	0
Jiangjin	−0.499	0.067	0.076	0.146	0.081	0.083	0.054	0.004
Kaizhou	−0.384	0.003	0.004	0.003	0.007	0.003	0.002	−0.001
Liangping	−0.861	0.13	0.161	−0.101	0.041	0.123	0.075	−0.191
Nanchuan	−0.995	0.4	0.259	0.167	0.183	0.198	0.14	−0.017
Qijiang	−0.311	0.145	0.431	0.18	0.215	0.397	0.126	−0.119
Rongchang	0	0	0	0	0	0	0	0
Shizhu	−2.285	−0.007	0.003	0.013	0.028	0.003	0.007	0.003
Tongliang	0	0	0	0	0	0	0	0
Tongnan	0	0	0	0	0	0	0	0
Wanzhou	−3.773	0.157	0.116	0.143	0.116	0.102	0.067	−0.063
Yongchuan	0	0	0	0	0	0	0	0
Yunyang	−2.663	−0.13	0.116	0.275	0.057	0.08	0.12	−0.041
Changshou	−0.184	−0.298	0.814	0.419	0.241	0.709	0.262	−0.138
Zhongxian	−1.13	0.278	0.124	0.181	0.159	0.08	0.08	−0.031
C-C E Zone	−0.325	0.055	0.106	0.084	0.079	0.097	0.04	−0.026

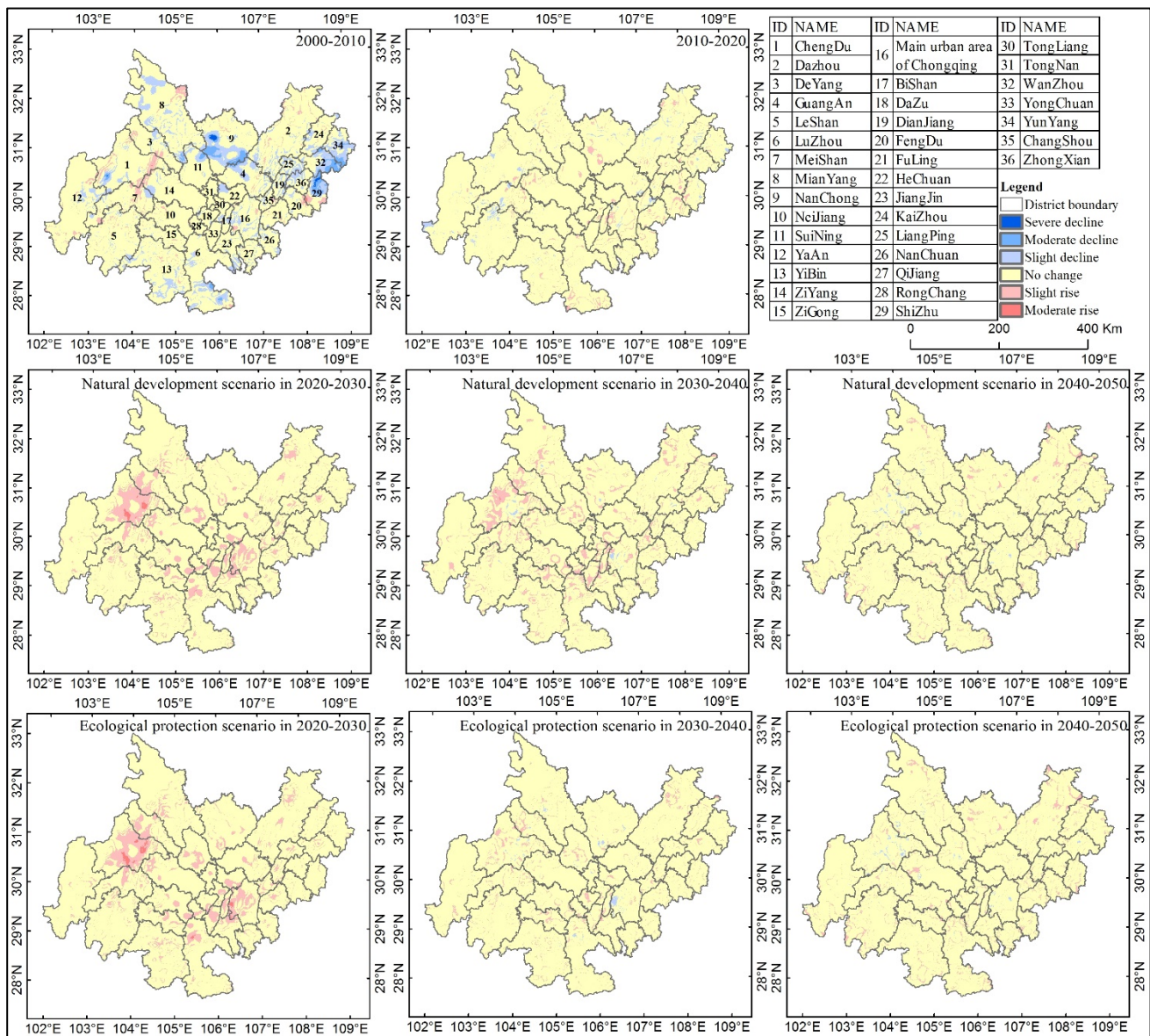


Figure 5. Evolution distribution of the LER level at the grid scale.

#### 4. Discussion

##### 4.1. The High-Precision Simulation Effect of the PLUS Model over a Wide Area Was Conducive to Analyzing Evolutionary Trends in LER

In this study, the PLUS model was introduced to simulate land use data for the C-C E Zone, and high-precision simulation results were obtained at a resolution of 30 m. The results were compared with the results of other land use simulation models, such as the CLUE-S model and CA-Markov model, which are widely used at present. For example, Islam et al. used the CLUE-S model to simulate land use data with a resolution of 30 m in Southeast Bangladesh, and the kappa coefficients were 0.61–0.71 [28]. Hu et al. used the CLUE-S and Markov models to simulate land use data with a resolution of 30 m in Beijing, and the kappa coefficient was greater than 0.75 [29]. Zhao et al. conducted a 30 m resolution land use simulation in Shunyi District of Beijing using a CA-Markov model, and the kappa coefficient was 0.77 [30]. These existing studies showed that the PLUS model has obvious advantages in its simulation range and accuracy, which was conducive to improving the accuracy of LER evolutionary trend analysis.

#### 4.2. Determination of the Ecological Grid Size Should Not Directly Refer to the Previous Research

In this study, the gradient division method ( $1 \times 1$  km,  $2 \times 2$  km, . . . ,  $10 \times 10$  km) was used to determine the optimal size of the ecological grid in the *LER* calculation, but this was rarely done in previous studies. The main reason was that in most studies, the size of the ecological grid was mostly determined by two to five times of the average plaque area in the study area or citing the research results of other scholars. For example, Yu et al. used the results of other scholars when calculating *LER* in Amu Darya Delta and selected  $5 \times 5$  km as the size of the ecological grid [31]. Based on the ecological risk research carried out by Tian et al. in Yongjiang River Basin of Zhejiang Province,  $2 \times 2$  km was determined as the ecological grid size based on 2–5 times the average plaque area in the study area [32]. The advantage of using this method to determine the optimal ecological grid size is that it was simple to operate and can reduce the amount of calculation. However, in the research of geography and ecology, it is obviously unscientific to use the same measurement standard in different regions, such as the obvious differences in terrain, elevation, and landscape fragmentation between plain and mountainous regions. At the same time, in our research, if the size of the ecological grid was determined as  $3 \times 3$  or  $5 \times 5$  km, the spatial distribution law of *LER* will not reflect the actual situation. Therefore, the gradient measurement method proposed in this study was scientific and reasonable for identifying the size of the best ecological grid.

#### 4.3. Development Scenario Research Will Help Reduce *LER* in the Future

In this study, we discussed the changes in *LER* under the *ND* and *EP* scenarios, and concluded that the *EP* scenario was conducive to reducing regional *LER*, which was related to the increase in the ecological land area and the control of construction land expansion under the *EP* scenario. Many studies have shown that social factors were important factors affecting *LER*. Yu et al. analyzed the influencing factors of *LER* in Amu Darya Delta and found that *LER* was higher in areas with a high population density [31]. Mondal et al. conducted an *LER* assessment study in Delhi and believed that incentives or services for urban development would put pressure on *LER* [6]. Chen et al. carried out *LER* assessment and driving force analysis in Peibei and found that the increase in the urbanization rate significantly improved *LER* [33]. Li et al. also concluded that human activities were the main reason affecting *LER* in Qinling area, and it was necessary to balance the relationship between economic development and environmental protection [1]. Under the *EP* scenario, due to the protection of ecological land and the reduced urban expansion rate, the *LER* will be effectively reduced compared with the *ND* scenario. This is consistent with the research conclusion of Xu et al., who used the Markov-FLUS model in Xinjiang, and the research shows that the *EP* scenario can significantly reduce the ecological risk compared with the *ND* scenario [34]. The multi scenario simulation carried out by Tian et al. in Yancheng coastal wetland also showed that the *LER* of the region can be significantly reduced under the *EP* scenario [35]. For this study, the regions with a high concentration of *LERI* (southeast of Mianyang, southeast of Deyang, east of Leshan, junction of Neijiang and Zigong, Yibin, Luzhou, south of Jiangjin, Qijiang, south of Banan, south of Fuling, Fengdu, north of Shizhu, north of Zhongxian, south of Wanzhou, south of Yunyang, etc.), the regions with a high level of *LERI* (Luzhou, Fuling, Yibin, Qijiang, Nanchuan, etc.), or regions with a rapid risk rise (Fuling, Fengdu, Changshou, etc.) should strengthen ecological protection and build a more reasonable combination of ecological space, living space, and production space.

#### 4.4. *LER* Can Explain Regional Ecological Risk at the Landscape Level

Ecological risk refers to the risk borne by the ecosystem and its components under the interference of natural or human activities. It is the possible adverse impacts of uncertain accidents or disasters on the structure and function of the ecosystem in a certain area. As an important branch of ecological risk assessment at the regional scale, *LER* refers to the possible adverse consequences of the interaction between landscape patterns and ecological processes under the influence of natural or human factors [36]. Therefore, *LER*

focuses on explaining regional ecological risk at the landscape level, which is similar to the approach in this study. It is generally believed that regions with a high level of economic development are regions with a high *LER*, and regions with a low economic development level are regions with a low *LER*. By measuring the *LER* of the *C-C E Zone*, this study found that the high level of economic development shows that the *LER* was low, especially in urban centers, such as Chengdu and the main urban areas of Chongqing. At the same time, the phenomenon of a higher *LER* was found in areas with low economic development levels, such as Yunyang, Qijiang, etc. We believe that this was because *LER* only considers the combination of landscape and the integrity of landscape patches. In the urban center, the landscape was mainly construction land. The landscape patches here were relatively complete, so they did not show a high *LER*. In areas with a low economic development level, the regional landscape was seriously various due to the cutting of cultivated plots and the loose distribution of rural settlements, so it shows a high *LER*. This was consistent with the *LER* analysis conducted by Chen et al. in Shiyang City [37] and Kang et al. in Manas River Basin [38]. This shows that an *LERI* can only represent the landscape level to judge the regional ecological risk and can be used to guide regional ecological risk prevention and control at the landscape level.

Therefore, this study constructed an *LERI* model composed of a landscape disturbance index and landscape vulnerability index. Although it provides a convenient and efficient evaluation method, and the use of this model was applicable to the *LER* evaluation based on land use change, it has less consideration of ecological processes, so it should be improved in the future for ecological risk assessment research

## 5. Conclusions

This research introduced the PLUS model, ecological grids, and the *LERI* model to analyze *LER* evolutionary trends in the *C-C E Zone* from 2000 to 2050 according to the *ND* and *EP* scenarios. The results showed that: (1) the PLUS model could obtain high-precision simulation results in the *C-C E Zone*. In the future, the increase rate in construction land area would be reduced, the declining rate of forest land and cultivated land area would also be reduced, and the area of various types of land would tend to be stable. (2) This study found that the optimal size of the ecological grid in the *LERI* calculation of the mountainous area was  $4 \times 4$  km. Moreover, the mean values of *LERI* in 2030, 2040, and 2050 were 0.1612, 0.1628, and 0.1636 for the *ND* scenario and 0.1612, 0.1618, and 0.1620 for the *EP* scenario. (3) The hot spot analysis results showed that an area of about 49,700 km<sup>2</sup> in the *C-C E Zone* from 2000 to 2050 belongs to high agglomeration of *LER*. (4) Since 2010, the proportions of high and extremely high risk levels have continued to increase, but under the *EP* scenario, the high and extremely high risk levels in 2040 and 2050 decreased from 14.36% and 6.66% to 14.33% and 6.43%. Regional analysis showed that the high and extremely high risk in most regions increased during 2010–2050. Moreover, the risk levels of Fuling, Fengdu, and Changshou increased for a long period of time, and the risk level increase rates of the three regions during 2000–2050 were 0.3196, 0.1994, and 0.1984, respectively. (5) Under the *ND* scenario, the proportions of grids with decreased, unchanged, and increased risk levels were 15.13%, 81.48%, and 3.39% for 2000–2010 and 0.54%, 94.75%, and 4.71% for 2040–2050. The proportion of grids with changed risk levels gradually decreased.

This study analyzed the evolutionary trends of *LER* in the *C-C E Zone* from 2000–2050 under the *ND* and *EP* scenarios. On the whole, the *LER* risk for the *C-C E Zone* showed an upward trend, and the ecological protection scenario was conducive to reducing the risk. The research results can serve as a valuable data reference set for regional landscape optimization and risk prevention and control. In the future, in order to manage *LER* prevention and control well, we should focus on ecological grids with a high *LERI* or rapid index rise, agglomeration areas with a high landscape risk, and areas with a high risk level or rapid rise in their level. Increasing the landscape layout at the macro level and landscape optimization at the micro level based on a landscape index is an effective way to reduce regional *LER*.

**Author Contributions:** Conceptualization, K.Z., J.H. and S.Z.; methodology, K.Z. and J.H.; software, K.Z., L.Z., L.W. and J.H.; formal analysis, K.Z. and L.W.; resources, K.Z. and J.H.; data curation, K.Z. and J.H.; writing—original draft preparation, K.Z. and Y.L.; writing—review and editing, K.Z. and S.Z.; visualization, K.Z. and J.H.; funding acquisition, K.Z., D.S. and S.Z. All authors have read and agreed to the published version of the manuscript.

**Funding:** This research was supported by Scientific Research Project of Chongqing Ecological Environment Bureau (No. CQEE-21C00364, No. CQEE2022-STHBZZ118), Special Project of Performance Incentive and Guidance for Scientific Research Institutions of Chongqing (No. Cqhky2021jxjl00001), Key Project of Humanities and Social Sciences Research of Chongqing Municipal Commission of Education (No. 22SKGH569).

**Institutional Review Board Statement:** Not applicable.

**Informed Consent Statement:** Not applicable.

**Data Availability Statement:** Not applicable.

**Conflicts of Interest:** The authors declare no conflict of interest.

## References

- Li, X.; Li, S.; Zhang, Y.; Connor, P.J.O.; Zhang, L.W.; Yan, J.P. Landscape Ecological Risk Assessment under Multiple Indicators. *Land* **2021**, *10*, 739. [[CrossRef](#)]
- Wu, Y.; Liu, H.; He, H. Stressors of dual-qualification nursing teachers in the ChengDu-ChongQing economic zone of China—a qualitative study. *Nurse Educ. Today* **2013**, *33*, 1496–1500. [[CrossRef](#)] [[PubMed](#)]
- Zhang, X.H.; Tao, H.; Wang, Y.J.; Ma, Z.Y.; Zhou, Z.Y. Pollution Characteristics and Risk Assessment of Tetracycline Antibiotics in Farmland Soil in Yinchuan. *Environ. Sci.* **2021**, *42*, 4933–4941.
- Wee, S.Y.; Omar, T.F.T.; Aris, A.Z.; Lee, Y. Surface Water Organophosphorus Pesticides Concentration and Distribution in the Langat River, Selangor, Malaysia. *Expo. Health* **2016**, *8*, 497–511. [[CrossRef](#)]
- Cui, L.; Zhao, Y.H.; Liu, J.C.; Han, L.; Ao, Y.; Yin, S. Landscape ecological risk assessment in Qinling Mountain. *Geol. J.* **2018**, *53*, 342–351. [[CrossRef](#)]
- Mondal, B.; Sharma, P.; Kundu, D.; Bansal, S. Spatio-temporal Assessment of Landscape Ecological Risk and Associated Drivers: A Case Study of Delhi. *Environ. Urban. Asia* **2021**, *12*, S85–S106. [[CrossRef](#)]
- Hunsaker, C.T.; Graham, R.L.; Suter, G.W.; Oneill, R.V.; Barnthouse, L.W.; Gardner, R.H. Assessing Ecological Risk on a Regional Scale. *Environ. Manag.* **1990**, *14*, 325–332. [[CrossRef](#)]
- Kityuttachai, K.; Tripathi, N.; Tipdecho, T.; Shrestha, R. CA-Markov analysis of constrained coastal urban growth modeling: Hua Hin seaside city. *Sustainability* **2013**, *5*, 1480–1500. [[CrossRef](#)]
- Kucsicsa, G.; Popovici, E.A.; Bălteanu, D.; Grigorescu, I.; Dumitrașcu, M.; Mitrică, B. Future land use/cover changes in romania: Regional simulations based on clue-s model and corine land cover database. *Landsc. Ecol. Eng.* **2019**, *15*, 75–90. [[CrossRef](#)]
- Liu, X.J.; Li, X.; Liang, X.; Shi, H.; Ou, J.P. Simulating the Change of Terrestrial Carbon Storage in China Based on the FLUS-InVEST Model. *Trop. Geogr.* **2019**, *39*, 397–409.
- Wu, D.; Zhu, K.W.; Zhang, S.; Huang, C.Q.; Li, J. Evolution Analysis of Carbon Storage in Chengdu-Chongqing Economic Zone Based on PLUS Model and InVEST Model. *Ecol. Environ. Monit. Three Gorges* **2021**, *7*, 1–18.
- Liang, X.; Liu, X.P.; Chen, G.L.; Leng, J.Y.; Wen, Y.Y.; Chen, G.Z. Coupling fuzzy clustering and cellular automata based on local maxima of development potential to model urban emergence and expansion in economic development zones. *Int. J. Geogr. Inf. Sci.* **2020**, *34*, 1930–1952. [[CrossRef](#)]
- Liang, X.; Guan, Q.F.; Clarke, K.C.; Liu, S.S.; Wang, B.Y.; Yao, Y. Understanding the drivers of sustainable land expansion using a patch-generating land use simulation (PLUS) model: A case study in Wuhan, China. *Comput. Environ. Urban Syst.* **2021**, *85*, 101569. [[CrossRef](#)]
- He, J.; Wu, L.J.; Zhang, L.X.; Chen, M.M. Landscape ecological risk assessment of Three Gorges Reservoir Area Based on Ecological Community. *Ecol. Environ. Monit. Three Gorges* **2022**, *25*, 1–19.
- Zeng, C.; He, J.; He, Q.Q.; Mao, Y.Q.; Yu, B.Y. Assessment of Land Use Pattern and Landscape Ecological Risk in the Chengdu-Chongqing Economic Circle, Southwestern China. *Land* **2022**, *11*, 659. [[CrossRef](#)]
- Liu, J.Y.; Ning, J.; Kuang, W.H.; Xu, X.L.; Zhang, S.W.; Yan, C.Z.; Li, R.D.; Wu, S.X.; Hu, Y.F.; Du, G.M.; et al. Spatio-temporal patterns and characteristics of land-use change in China during 2010–2015. *Acta Geogr. Sin.* **2018**, *73*, 789–802.
- Wang, F.; Ye, C.S.; Hua, J.Q.; Li, X. Coupling Relationship between Urban Spatial Expansion and Landscape Ecological Risk in Nanchang City. *Acta Ecol. Sin.* **2019**, *39*, 1248–1262.
- Bai, S.T. Study on Landscape Ecological Risk Assessment of Western Jilin Based on Land Use Change. Master’s Thesis, Jilin University, Jilin, China, 2019.
- Du, J.; Zhao, S.C.; Qiu, S.K.; Guo, L. Land use change and landscape ecological risk assessment in loess hilly region of western Henan Province from 2000 to 2015. *Res. Soil Water Conserv.* **2021**, *28*, 279–284.

20. Hou, R.; Li, H.B.; Gao, Y.L. Ecological risk assessment of land use in Jiangxia district of Wuhan based on landscape pattern. *Res. Soil Water Conserv.* **2021**, *28*, 323–330.
21. Shen, H.C.; Xue, L.Q. Landscape Ecological Risk Assessment of the Lower Reaches of Tarim River Based on Land Use Change in Recent 20 Years. *China Rural. Water Hydropower* **2020**, *11*, 77–82.
22. Qing, Q.L.; Huang, Y.; Pei, C. Eco-risk assessment and management based on landscape structure changes—A case study of Wanzhou district of Chongqing. *J. Southwest Univ.* **2021**, *43*, 174–184.
23. Yang, K.; Xin, G.X.; Jiang, H.Y.; Yang, C.X. Study on spatiotemporal changes of landscape ecological risk based on the optimal spatial scale: A case study of Jiangjin district, Chongqing city. *J. Ecol. Rural. Environ.* **2021**, *37*, 576–586.
24. Rangel-Buitrago, N.; Neal, W.J.; de Jonge, V.N. Risk assessment as tool for coastal erosion management. *Ocean. Coast. Manag.* **2020**, *186*, 105099. [[CrossRef](#)]
25. Lou, N.; Wang, Z.J.; He, S.T. Assessment on Ecological Risk of Aha Lake National Wetland Park Based on Landscape Pattern. *Res. Soil Water Conserv.* **2020**, *27*, 233–239.
26. Cui, Y.L.; Gao, X.; Dong, B.; Wei, H.M. Landscape ecological risk assessment of county. *J. Zhejiang AF Univ.* **2021**, *38*, 541–551.
27. Zhu, K.W.; Yang, Z.M.; Huang, L.; Chen, Y.C.; Zhang, S.; Xiong, H.L.; Wu, S.; Lei, B. Coupling ITO3dE model and GIS for spatiotemporal evolution analysis of agricultural non-point source pollution risks in Chongqing in China. *Sci. Rep.* **2021**, *11*, 1–18. [[CrossRef](#)]
28. Islam, S.; Li, Y.C.; Ma, M.G.; Chen, A.X.; Ge, Z.X. Simulation and Prediction of the Spatial Dynamics of Land Use Changes Modelling Through CLUE-S in the Southeastern Region of Bangladesh. *J. Indian Soc. Remote Sens.* **2021**, *49*, 2755–2777. [[CrossRef](#)]
29. Hu, Y.C.; Zheng, Y.M.; Zheng, X.Q. Simulation of land-use scenarios for Beijing using CLUE-S and Markov composite models. *Chin. Geogr. Sci.* **2013**, *23*, 92–100. [[CrossRef](#)]
30. Zhao, D.L.; Du, M.; Yang, J.Y.; Li, P.S.; He, S.S.; Zhu, D.H. Simulation and Forecast Study of Land Use Change Based on CA-Markov Model. *Trans. Chin. Soc. Agric. Mach.* **2016**, *47*, 278–285.
31. Yu, T.; Bao, A.; Xu, W.; Guo, H.; Jiang, L.; Zheng, G. Exploring variability in landscape ecological risk and quantifying its driving factors in the amu darya delta. *Int. J. Environ. Res. Public Health* **2020**, *17*, 79. [[CrossRef](#)]
32. Tian, P.; Li, J.; Gong, H.; Pu, R.; Liu, R. Research on land use changes and ecological risk assessment in yongjiang river basin in zhejiang province, china. *Sustainability* **2019**, *11*, 2817. [[CrossRef](#)]
33. Chen, X.Q.; Ding, Z.Y.; Yang, J.; Chen, X.D.; Chen, M.N. Ecological risk assessment and driving force analysis of landscape in the compound mine-urban area of the northern Peixian County. *Chin. J. Ecol.* **2022**, *41*, 1–11.
34. Xu, Q.; Guo, P.; Jin, M.; Qi, J. Multi-scenario landscape ecological risk assessment based on markov-flus composite model. *Geomat. Nat. Hazards Risk* **2021**, *12*, 1448–1465. [[CrossRef](#)]
35. Tian, P.; Cao, L.; Li, J.; Pu, R.; Gong, H.; Li, C. Landscape characteristics and ecological risk assessment based on multi-scenario simulations: A case study of yancheng coastal wetland, China. *Sustainability* **2020**, *13*, 149. [[CrossRef](#)]
36. Jian, Q.; Zhang, L.Q.; Zhang, P.T.; Zhao, L. Study on Landscape Ecological Risk Assessment and Spatial Differentiation of Qinglong Manchu Autonomous County Based on Explicit and Implicit Analysis. *Res. Soil Water Conserv.* **2018**, *25*, 228–235.
37. Chen, Y.H.; Yu, J.; Nie, Y.; Tang, B.; Liu, C.C. Spatial Coupling Between Land Use Level and Landscape Ecological Risk—Taking Shiyan City as an Example. *Res. Soil Water Conserv.* **2021**, *28*, 285–291+2.
38. Kang, Z.W.; Zhang, Z.Y.; Wei, H.; Liu, L.; Ning, S.; Zhao, G.N.; Wang, T.X.; Tian, H. Landscape ecological risk assessment in Manas River Basin based on land use change. *Acta Ecol. Sin.* **2020**, *40*, 6472–6485.